





RESEARCH ARTICLE OPEN ACCESS

Synthesis of Aromatic Aldehydes by C–H Formylation of Aromatics with Silyl Formates Prepared from CO₂ and Hydrosilanes

 Natsumi Nitta¹  | Kei Hirokawa¹ | So Saibara¹ | Bikash Dev Nath^{1,2}  | Kazuto Takaishi¹  | Tadashi Ema¹ 
¹Graduate School of Environmental, Life, Natural Science and Technology, Okayama University, Okayama, Japan | ²Department of Chemistry, Dhaka University of Engineering & Technology, Gazipur, Bangladesh

Correspondence: Natsumi Nitta (nitta@okayama-u.ac.jp) | Tadashi Ema (ema@cc.okayama-u.ac.jp)

Received: 24 October 2025 | **Revised:** 12 May 2026 | **Accepted:** 19 May 2026

Keywords: aldehydes | carbon dioxide fixation | CO₂ reduction | formylation | hydrosilylation

ABSTRACT

Despite the recent remarkable progress in CO₂ fixation reactions, the methods for the synthesis of aldehydes from CO₂ are quite limited partly because of the lability of the resulting formyl group and difficulty in the controlled deoxygenative CO₂ conversions leading to C–H and C–C bond formation. Here, we have developed the direct C–H formylation of electron-rich aromatics using silyl formates, prepared from CO₂ and hydrosilanes, in the presence of BCl₃ or BBr₃. This is the first report on the direct C–H formylation of aromatics with silyl formates. Useful compounds including a biologically active compound and octaethylporphyrin were synthesized by fixing one to four CO₂ molecules in a stepwise manner. DFT calculations have been done to elucidate the reaction mechanism including a dual role of BBr₃ in the activation of silyl formate, HCO₂SiMe₂Ph, and electrophilic aromatic substitution.

1 | Introduction

Aromatic aldehydes constitute an important class of compounds, having various applications such as synthetic intermediates for drugs and functional compounds [1–3]. Although the Gattermann–Koch reaction, Reimer–Tiemann reaction, Duff reaction, and Vilsmeier–Haack reaction are widely known as conventional synthetic methods for aromatic aldehydes [4–7], they have drawbacks such as the use of toxic gases, limited substrate scope, and severe reaction conditions. Therefore, much efforts have been made to develop green and sustainable methods for the synthesis of aromatic aldehydes [8–10].

Carbon dioxide (CO₂) is a sustainable C1 source because of abundance, renewability, and inexpensiveness, and the chemical fixation of CO₂ is a hot topic despite the kinetic and thermodynamic stability of CO₂ [11–17]. Among various CO₂ fixation reactions, reductive CO₂ conversions play a pivotal role in accessing a wide

range of organic compounds [18–22]. Various reductants can be used such as H₂ [23], hydrosilanes [24–26], and hydroboranes [27]. Among them, hydrosilanes are especially useful because they show moderate reactivity and stability in air and because deoxygenative CO₂ conversions can be driven by the formation of the strong Si–O bond. The stepwise reduction of CO₂ with hydrosilanes takes place, generating silyl formates (HCO₂Si), bis(silyl)acetals (SiOCH₂OSi), methoxysilanes (CH₃OSi), and methane [28–34], some of which can be used as reactive species for the synthesis of value-added organic compounds [35–44].

The formation of the formyl group from CO₂ is a challenging subject partly because aldehydes are labile under severe reaction conditions and because the deoxygenative transformation of CO₂ is involved. In fact, the examples of aldehyde synthesis with CO₂ are quite limited [45–56]. For example, the transition metal-catalyzed formylation of aryl halides and hydroformylation of olefins have been reported [45–53]. In most cases, CO₂ is converted

This is an open access article under the terms of the [Creative Commons Attribution-NonCommercial-NoDerivs](https://creativecommons.org/licenses/by-nc-nd/4.0/) License, which permits use and distribution in any medium, provided the original work is properly cited, the use is non-commercial and no modifications or adaptations are made.

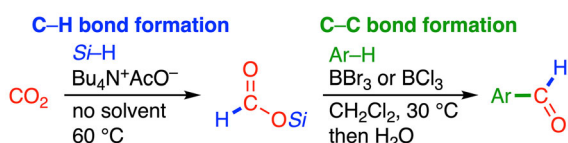
© 2026 The Author(s). *Advanced Synthesis & Catalysis* published by Wiley-VCH GmbH.

in situ into CO, which is successively used in the C–C bond formation. On the other hand, we have reported the methods for the two-step synthesis of aldehydes with CO₂ and hydrosilanes; a C–H bond is formed in the first step, and a C–C bond is formed in the second step [54–56]. For example, the *N*-formylation of amines with CO₂ and PhSiH₃ using tetrabutylammonium acetate (TBAA) or Cu(OAc)₂ as a catalyst under solvent-free conditions afforded Weinreb formamide or Comins–Meyers formamide, which were used for the one-pot synthesis of aldehydes by the reaction with Grignard reagents. In addition, *N*-methylformanilide was synthesized from *N*-methylaniline, CO₂, and PhSiH₃ using TBAA and Cu(OAc)₂ as catalysts under solvent-free conditions and was used in the one-pot Vilsmeier–Haack reaction to synthesize aromatic aldehydes. However, these reactions have a drawback of poor atom economy; the amines react with silyl formates to give formamides, which are then converted into aldehydes, giving off the amines as wastes. Here, we have developed the direct C–H formylation of aromatics using silyl formates synthesized from CO₂ and hydrosilanes (Scheme 1), which is an amine-free system with better atom economy. To the best of our knowledge, this is the first report on the direct C–H formylation of aromatics with silyl formates prepared from CO₂ and hydrosilanes. This reaction is promoted by BBr₃ or BCl₃ under mild conditions using no precious or transition metals. The reaction mechanism including the roles of silyl formates and Lewis acids has been elucidated by density functional theory (DFT) calculations.

2 | Results and Discussion

2-Naphthol (**1a**) was allowed to react with HCO₂SiMe₂Ph (3 equiv.), which was prepared from CO₂ (balloon) and PhMe₂SiH using TBAA (5 mol%) as a catalyst under solvent-free conditions [54], in the presence of a Lewis acid (3 equiv.) at 30°C for 6 h (Table 1). 2-Hydroxy-1-naphthaldehyde (**2a**) was obtained in 100% and 96% yield when BBr₃ and BCl₃ (3 equiv.) were used as Lewis acids, respectively (entries 1 and 2). In sharp contrast, a trace amount of **2a** was obtained when BF₃·OEt₂, TiCl₄, or CH₃SO₃H were used as a Lewis/Brønsted acid, and no reaction took place when the following acids were used: AlCl₃, Sc(OTf)₃, ZnCl₂, Zn(OTf)₂, Y(OTf)₃, InCl₃, SnCl₄, TMSCl, TMSOTf, CF₃SO₃H, or Me₃O⁺BF₄[−] (entries 7 and 8). A decrease in the amount of BBr₃ or BCl₃ resulted in a drop in the yield (entries 3–6). Based on these results, the use of BBr₃ or BCl₃ (2–3 equiv.) is suitable for this reaction, and BBr₃ appears to be more active than BCl₃. The fact that only BBr₃ and BCl₃ promoted the formylation suggests that there is a reaction mechanism specific to BBr₃ and BCl₃ as described later.

We also examined the effect of silyl formates (Table 2). When HCO₂SiMe₂Ph, HCO₂SiMePh₂, and HCO₂SiPh₃ were used as a



SCHEME 1 | C–H formylation of aromatics with silyl formates derived from CO₂.

TABLE 1 | Synthesis of aldehyde **2a** by the reaction of **1a** with HCO₂SiMe₂Ph.

Entry ^a	Acid (X equiv.)	Yield (%) ^b
1	BBr ₃ (3)	100
2	BCl ₃ (3)	96
3	BBr ₃ (2)	83
4	BCl ₃ (2)	61
5	BBr ₃ (1)	Trace
6	BCl ₃ (1)	Trace
7	BF ₃ ·OEt ₂ (3) ^c	Trace
8	AlCl ₃ (3) ^d	0

^aReaction conditions: **1a** (0.3 mmol), HCO₂SiMe₂Ph (crude, 0.9 mmol), Lewis/Brønsted acid (amount indicated above), CH₂Cl₂ (0.9 mL), 30°C, 6 h, then H₂O.

^bNMR yield of **2a**.

^cThe same results with TiCl₄ or CH₃SO₃H.

^dThe same results with Sc(OTf)₃, ZnCl₂, Zn(OTf)₂, Y(OTf)₃, InCl₃, SnCl₄, TMSCl, TMSOTf, CF₃SO₃H, or Me₃O⁺BF₄[−].

TABLE 2 | Screening of hydrosilanes.

Entry ^a	Step 1		Step 2	
	Silyl formate	Yield (%) ^b	Yield (%) ^b	
1	HCO ₂ SiMe ₂ Ph	70	100 (84) ^c	(53) ^d
2	HCO ₂ SiMePh ₂	45	90	
3	HCO ₂ SiPh ₃	35	24	
4 ^e	(HCO ₂) _n Si(H) _{3-n} Ph	40	0	

^aReaction conditions: **1a** (0.3 mmol), silyl formate (crude, 0.9 mmol), BBr₃ (0.9 mmol, 1 M in CH₂Cl₂), 30°C, 6 h, then H₂O.

^bNMR yield.

^cHCO₂SiMe₂Ph (crude, 0.6 mmol).

^dHCO₂SiMe₂Ph (crude, 0.3 mmol).

^e30°C in step 1, 2 h. *n* = 1–3.

formyl source, **2a** was obtained in 100%, 90%, and 24% yield, respectively (entries 1–3). HCO₂SiMe₂Ph was more productive than HCO₂SiMePh₂ or HCO₂SiPh₃ probably because the former was sterically less hindered. On the other hand, the use of silyl formates prepared from PhSiH₃ did not afford **2a** at all (entry 4), which suggests that silyl formates bearing the primary silicon

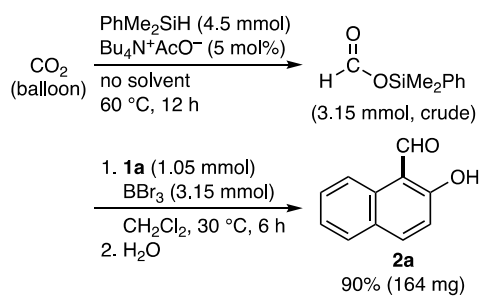
atom were decomposed during the reaction. Since the reaction of **1a** with 1 or 2 equivalent of HCO₂SiMe₂Ph afforded **2a** in lower yields (53–84%) (entry 1), the use of 3 equivalent of HCO₂SiMe₂Ph was found to be the best. A one-pot reaction was conducted on a 1 mmol scale (Scheme 2). HCO₂SiMe₂Ph (3.15 mmol) was synthesized from CO₂ and PhMe₂SiH (4.5 mmol) in 70% yield as determined by nuclear magnetic resonance (NMR) spectroscopy, and **1a** (1.05 mmol) and BBr₃ (3.15 mmol) were then added to the solution, and **2a** was obtained in 90% yield.

BBr₃ and BCl₃ are common reagents frequently used for the cleavage of the alkoxy group [57, 58]. To examine the effect of BBr₃ and BCl₃ on the alkoxy group, 2-methoxynaphthalene (**1d**) was subjected to the standard reaction (Scheme 3). As a result, BBr₃ effected both formylation and demethylation to deliver **2a** in 94% yield, while BCl₃ promoted the selective formation of 2-methoxy-1-naphthaldehyde (**2d**) in 66% yield, which indicates that BCl₃ is suitable for substrates having alkoxy groups.

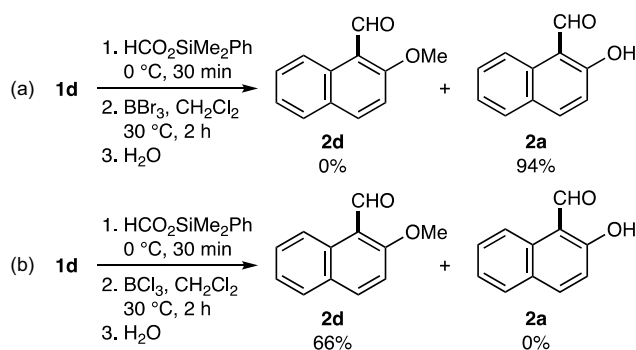
We investigated substrate scope under the optimized reaction conditions mainly using HCO₂SiMe₂Ph and BCl₃ (Table 3). As a result, aldehydes **2a**, **2b**, and **2c** with the hydroxy group were isolated in 92%, 52%, and 49% yield, respectively. The yield of **2b** could be improved by shortening the reaction time to 2 h, which suppressed the formation of insoluble materials. As for substrates **1d**, **1e**, and **1f** with the alkoxy group, the reaction time was set to 2 h to suppress the cleavage of the alkoxy group, and **2d**, **2e**, and **2f** were obtained in 61%, 44%, and 54%, respectively. Anthracene (**1g**) was successfully converted into **2g** in 77% yield. Although pyrene (**1h**) was converted into **2h** in 32% yield under the standard reaction conditions, the use of HCO₂SiMePh₂ and BBr₃

instead of HCO₂SiMe₂Ph and BCl₃ increased the production of **2h** to 65% yield. In the case of perylene (**1i**), aldehyde **2i** was obtained in 58% yield by extending reaction time from 6 h to 24 h. Azulene (**1j**) was converted into **2j** in only 34% yield probably because of instability, and the yield could not be improved by changing the reaction conditions. Indoles **1k** and **1l** were transformed to **2k** and **2l** in 71% and 77%, respectively. When carbazole (**1m**) was used as a substrate, not aldehyde but *N*-formylated product **2m'** was obtained in 86% yield. 9-Methylcarbazole (**1n**) was successfully converted into aldehyde **2n** in 53% yield. The use of HCO₂SiMePh₂ in place of HCO₂SiMe₂Ph enabled the synthesis of **2n** in 94% yield, while the use of HCO₂SiMePh₂ and BBr₃ in place of HCO₂SiMe₂Ph and BCl₃ afforded **2n** in 74% yield. The moderate bulkiness of HCO₂SiMePh₂ and the moderate Lewis acidity of BCl₃ may suppress overreactions, leading to the improvement of the reaction yield. Ferrocene (**1o**) was a good substrate, and aldehyde **2o** was obtained in 90% yield. We employed 2,2'-biindoles **1p** and **1q** to aim for double C–H formylation. Although **1p** with the NH groups was converted into dialdehyde **2p** in a low yield, **1q** with the *N*-methyl groups was successfully converted by BBr₃ into dialdehyde **2q** in 79% yield.

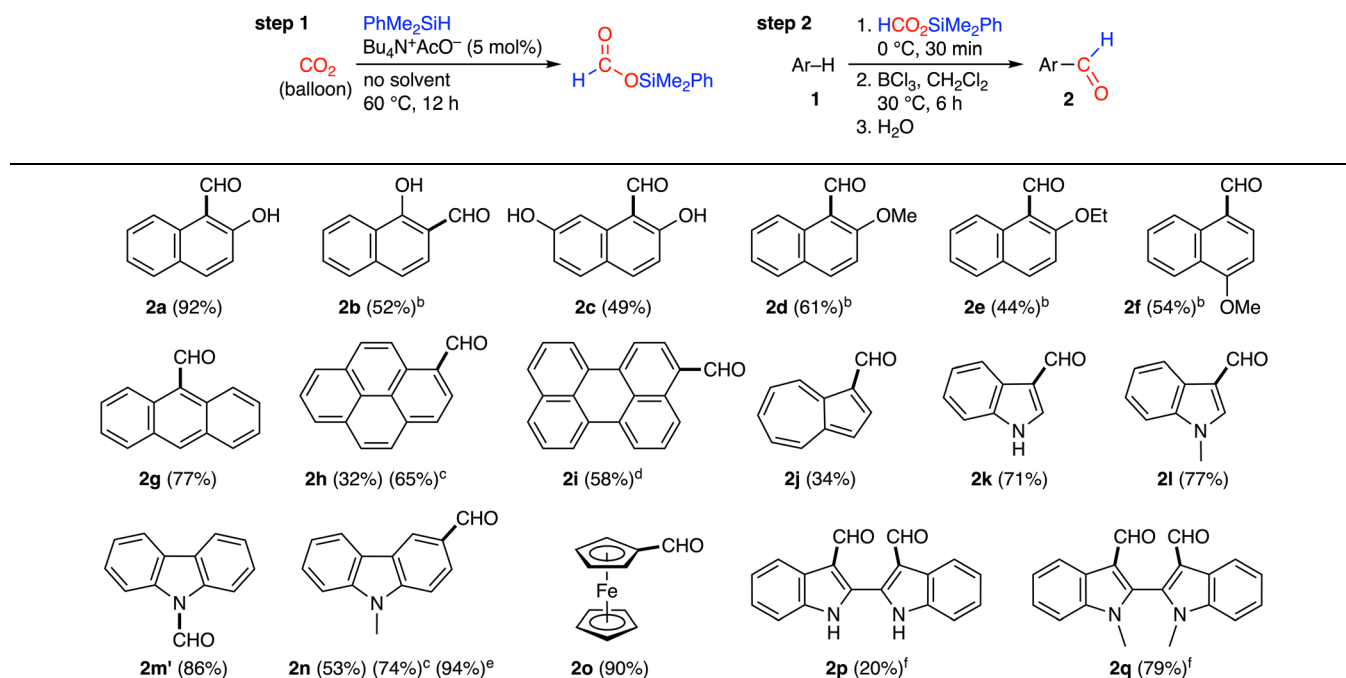
We applied the present method to the synthesis of biologically active compound, 5,11-dimethylindolo[3,2-*b*]carbazole-6-carboxaldehyde (**2r**) (Scheme 4a). **2r** is known as an agonist for the aryl hydrocarbon receptor (AhR) [59]. The binding of **2r** to AhR induces the translocation of AhR from the cytoplasm into the nucleus and then the formation of a heterodimer with ARNT (AhR nuclear translocator), leading to the binding to specific DNA sequences in the promoter regions and the transcription of genes such as CYP1A1. Based on the assay with ethoxyresorufin-*O*-deethylase, **2r** was found to show 39-fold activity relative to blank even at a low concentration of 80 nM [59]. We synthesized 5,11-dimethylindolo[3,2-*b*]carbazole (**1r**) from 1-methylindole (**1i**), CO₂, and PhSiH₃ using BPh₃ as a catalyst in acetonitrile at 40°C as reported previously [60], and **1r** was then subjected to C–H formylation. As a result, AhR agonist **2r** with three CO₂ molecules fixed, regioisomer **2r'**, and diformyl derivative **2r''** with four CO₂ molecules fixed were obtained in 14%, 35%, and 8% yield, respectively. This modest regioselectivity probably originated from the comparable electron-rich sites at the 2-, 6-, 8-, and 12-positions of the indolo[3,2-*b*]carbazole framework, and the two formyl groups were attached to the 2- and 8-positions, forming **2r''**, because these two sites are distant enough. To further understand this reaction, the Vilsmeier–Haack reaction of **1r** was also done for comparison (Scheme 4c) [61]. The Vilsmeier–Haack reaction of **1r** with *N*-methylformanilide and POCl₃ produced **2r** and **2r'** in 26% and 36% yield, respectively, without formation of **2r''**. The fact that **2r''** was produced only in the present method suggests that a reactive species made up of HCO₂SiMe₂Ph and BBr₃ is more electrophilic than the Vilsmeier reagent. On the other hand, the fact that the selectivity of **2r** over **2r'**/**2r''** was lower in the present method than in the Vilsmeier–Haack reaction performed at higher temperature suggests that the reactive species made up of HCO₂SiMe₂Ph and BBr₃ is bulkier than the Vilsmeier reagent because the 6- and 12-positions are more sterically hindered than the 2- and 8-positions. We also synthesized 2,5,8,11-tetramethylindolo[3,2-*b*]carbazole (**1s**) from 1,5-dimethylindole, CO₂, and PhSiH₃ in the same way [60], and **1s** was used as a substrate for the direct C–H formylation (Scheme 4b). As a result,



SCHEME 2 | One-pot synthesis of **2a** on a 1 mmol scale.



SCHEME 3 | Difference in reactivity and outcome between (a) BBr₃ and (b) BCl₃.

TABLE 3 | C–H formylation of aromatics.^a

^aReaction conditions: **1** (0.3 mmol), $\text{HCO}_2\text{SiMe}_2\text{Ph}$ (crude, 0.9 mmol), BCl_3 (0.9 mmol, 1 M in CH_2Cl_2), 30 °C, 6 h. Isolated yields of **2**.

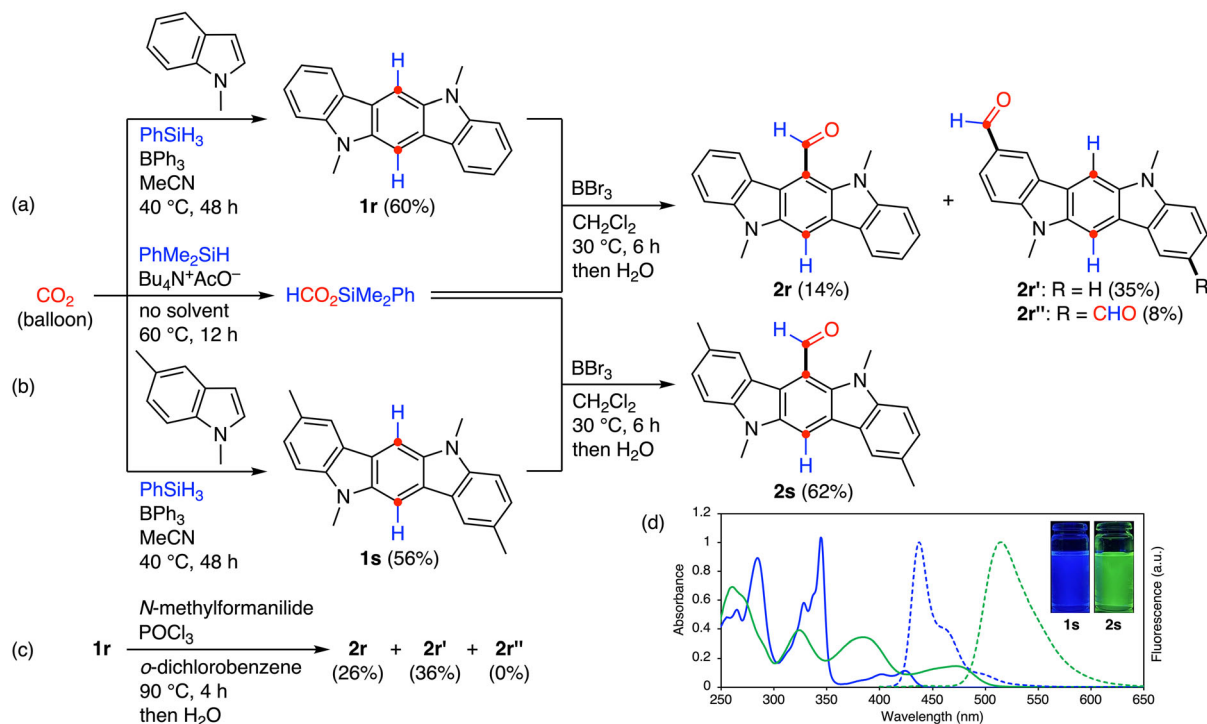
^b2 h.

^c $\text{HCO}_2\text{SiMePh}_2$ and BBr_3 instead of $\text{HCO}_2\text{SiMe}_2\text{Ph}$ and BCl_3 .

^d24 h.

^e $\text{HCO}_2\text{SiMePh}_2$ instead of $\text{HCO}_2\text{SiMe}_2\text{Ph}$.

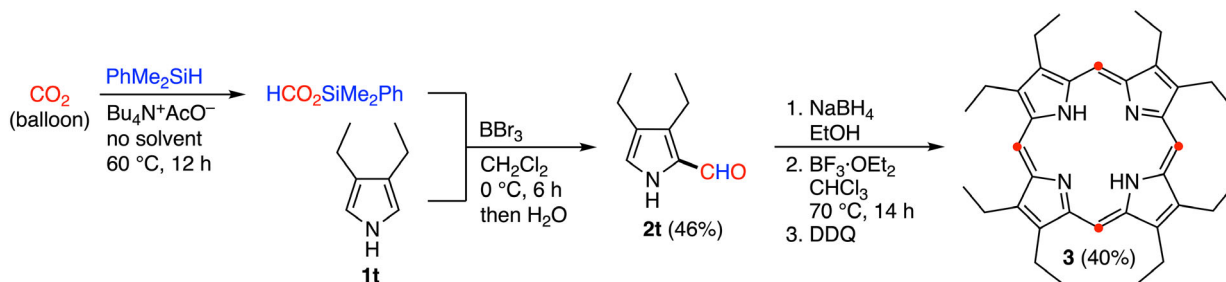
^f**1** (0.15 mmol), BBr_3 instead of BCl_3 .



SCHEME 4 | Synthesis of (a) biologically active substance **2r** and (b) analog **2s** by the sequential CO_2 fixation reactions. (c) The Vilsmeier–Haack reaction of **1r** for comparison. (d) UV-vis absorption spectra (solid line) and fluorescence spectra (dotted line) of **1s** (blue) and **2s** (green) in DMSO (2.0×10^{-5} M). $\lambda_{\text{ex}} = 395$ nm. Photographs of solutions of **1s** and **2s** in DMSO under UV light (365 nm) are also shown.

2,5,8,11-tetramethylindolo[3,2-*b*]carbazole-6-carboxaldehyde (**2s**) was selectively obtained in 62% yield. Fortunately, **2s** was stable under air despite the possession of the formyl group probably

because of steric protection. **2s** showed absorption and fluorescence bands at longer wavelengths than **1s**, and almost colorless and slightly yellow solutions of **1s** and **2s** in DMSO exhibited blue



SCHEME 5 | C–H formylation of 3,4-diethylpyrrole (**1t**) and the transformation of the resulting 2-formylpyrrole **2t** to porphyrin **3**.

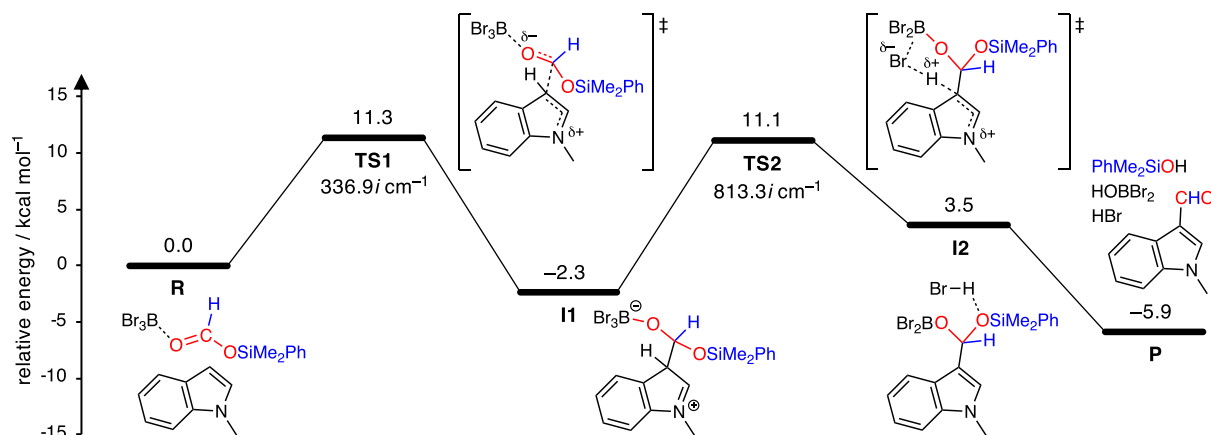


FIGURE 1 | Energy profile for the C–H formylation of 1-methylindole (**1I**). Relative free energies (303 K) are shown in kcal mol⁻¹. DFT calculations were performed at the ωB97XD/6-31G(d) level of theory. The self-consistent reaction field (SCRf) method with the polarizable continuum model (PCM) was adopted to take the solvation effect into account, and the PCM parameters for dichloromethane were employed. The energy of H₂O is included in the former steps where it does not appear explicitly in the computational model.

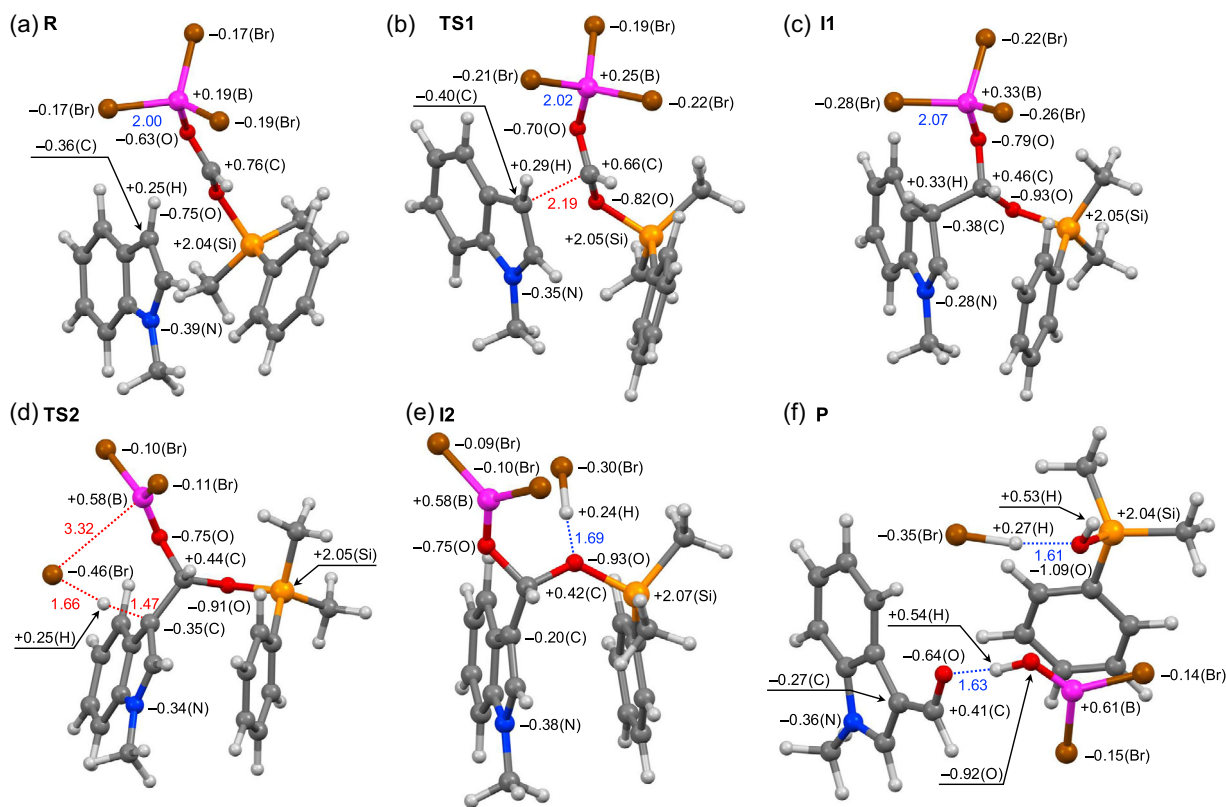


FIGURE 2 | DFT-optimized structures of (a) **R**, (b) **TS1**, (c) **I1**, (d) **TS2**, (e) **I2**, and (f) **P**. Distances (Å) are shown in blue or red, and natural bond orbital (NBO) charges are shown in black.

and green fluorescence, respectively, upon UV light irradiation under dark (Scheme 4d). These aldehydes **2r**, **2r'**, **2r''**, and **2s** are potential precursors for optoelectronic materials since the derivatization of similar compounds has previously been reported [62, 63].

Because porphyrins and metalloporphyrins are important and useful pigments showing unique physicochemical properties, catalytic activities, and supramolecular behaviors, we decided to construct the porphyrin framework using CO₂ as a building block. 3,4-Diethylpyrrole (**1t**) was converted into aldehyde **2t** at 0°C in 46% yield, and the reduction of **2t** with NaBH₄ followed by the macrocyclization of the resulting alcohol and oxidation with DDQ afforded 2,3,7,8,12,13,17,18-octaethylporphyrin (**3**) with four CO₂ molecules fixed in the π system (Scheme 5). Since several aromatic aldehydes shown in Table 3, such as **2a** and **2h**, have previously been used for the synthesis of *meso*-aryl-substituted porphyrins [64, 65], the formal synthesis of them with CO₂ has been achieved.

To elucidate the reaction mechanism, we performed DFT calculations on the reaction of 1-methylindole (**1l**) with HCO₂SiMe₂Ph in the presence of BBr₃ and obtained an energy diagram as shown in Figure 1. All the DFT-optimized structures including the intermediate and transition-state structures are presented in Figure 2. Binding of BBr₃ to HCO₂SiMe₂Ph forms an activated species, which triggers the formation of zwitterionic Wheland intermediate **I1** via transition state **TS1** with a ΔG^\ddagger value of 11.3 kcal mol⁻¹. In **TS1**, the newly forming C—C bond is relatively long (2.19 Å), and the carbon atom of the carbonyl group is close to sp² hybridization rather than sp³ hybridization. Upon transformation of **R** into **I1**, the positive charge on the boron atom increases, and the negative charge on the bromine atoms increases. The resulting intermediate **I1** is then converted into intermediate **I2** via **TS2** with a ΔG^\ddagger value of 13.4 kcal mol⁻¹. The proton at the 3-position is abstracted by the negatively charged bromine atom released from the boron atom in **TS2**. In this way, BBr₃ has two roles: the Lewis acid for the activation of HCO₂SiMe₂Ph and the base (Br⁻) for the proton abstraction. The resulting HBr forms a hydrogen bond with the oxygen atom of the siloxy group of **I2**, where π - π stacking occurs between the indole ring and the phenyl group with the shortest distance of 3.32 Å. Finally, **I2** is hydrolyzed to deliver the aldehyde product. Considering that both transition states (**TS1** and **TS2**) have small ΔG^\ddagger values and that the whole reaction of the C—H formylation is exothermic, this reaction is likely to occur at ambient temperature.

3 | Conclusion

Various synthetic methods for CO₂ fixation are required to create more sustainable societies. It is still difficult to convert CO₂ into the formyl group partly because CO₂ needs to undergo both C—H and C—C bond formation. Here, we have developed the method for the synthesis of aromatic aldehydes by the direct C—H formylation of electron-rich aromatics using silyl formates prepared from CO₂ and hydrosilanes in the presence of BCl₃ or BBr₃. This is the first example of the C—H formylation of aromatics with silyl formates derived from CO₂, and good substrate scope was confirmed. Useful compounds including a biologically active compound and octaethylporphyrin were synthesized by fixing

one to four CO₂ molecules in a stepwise manner. Because of the synthetic utility of aldehydes, the further derivatization of CO₂-derived aldehydes will be possible. Further study is under way to develop sustainable organic synthesis based on effective and efficient CO₂ fixation.

4 | Experimental Section

4.1 | General Procedure for the Synthesis of Aldehydes with CO₂

4.1.1 | Step 1. Synthesis of Silyl Formate

In a glovebox (purge type) under N₂ atmosphere, TBAA (68 mg, 0.23 mmol, 5 mol%) was put in a 30 mL Schlenk flask (dried at 150°C for a few hours and cooled down) fitted with a magnetic stirring bar and a rubber septum, and the flask was taken out from the glovebox. After the flask was evacuated and filled with CO₂ (balloon), PhMe₂SiH (696 μ L, 4.5 mmol, stored over molecular sieves 3A) was added via a syringe. The reaction mixture was stirred at 60°C for 12 h and cooled to room temperature to give a crude solution (ca. 700 μ L) containing HCO₂SiMe₂Ph, which was used in the subsequent reaction without purification. 1,2-Dichloroethane (39 μ L, 0.50 mmol) was added as an internal standard to quantify the amount of HCO₂SiMe₂Ph by means of ¹H NMR spectroscopy (typically, 70% NMR yield).

4.1.2 | Step 2. Synthesis of Aldehyde

To a 5 mL two-neck round-bottom flask (dried at 150°C for a few hours and cooled down) fitted with a magnetic stirring bar and a rubber septum, aromatic substrate **1** (0.30 mmol) was added, and the flask was quickly evacuated and filled with N₂ (balloon). The reaction mixture obtained in step 1 (200 μ L) containing HCO₂SiMe₂Ph (0.90 mmol, 3 equiv.) was added to the flask via a syringe, and the mixture was stirred at 0°C for 30 min. A solution of BCl₃ or BBr₃ (1 M solution in CH₂Cl₂, 0.9 mL, 0.90 mmol, 3 equiv.) was added. The mixture was stirred at 30°C for 6 h. The mixture was cooled in an ice bath, and the reaction was quenched with water (3 mL). The mixture was neutralized with saturated aqueous NaHCO₃ (3 mL). The product was extracted with CH₂Cl₂ (10 mL \times 2). The organic layers were combined, washed with water (10 mL), and dried over Na₂SO₄. After the evaporation of the solvent, mesitylene (14 μ L, 0.10 mmol) was added as an internal standard to quantify the amount of the product by means of ¹H NMR spectroscopy. Purification by silica gel column chromatography gave aldehyde **2**.

Acknowledgments

This work was supported by JSPS KAKENHI (grant no. 20H02780 and 24K01488) and Okayama Foundation for Science and Technology. This work was also supported by JSPS Program for Forming Japan's Peak Research Universities (J-PEAKS) grant number JPJS00420230010. We thank Division of Instrumental Analysis, Okayama University for the measurements of NMR spectra. The computations were carried out at RCCS (Okazaki, Japan) (Project: 25-IMS-C098 and 26-IMS-C091).

Funding

This study was supported by JSPS KAKENHI (20H02780, 24K01488), Okayama Foundation for Science and Technology, and JSPS Program for Forming Japan's Peak Research Universities (JPJS00420230010).

Conflicts of Interest

The authors declare no conflicts of interest.

Data Availability Statement

The data that support the findings of this study are available in the supplementary material of this article.

References

1. A. Kherudkar, A. Bhattacharjee, A. Nawkhare, S. Mukherjee, S. Pramanick, and J. K. Laha, "Recent Advances on Direct Formylation Reactions," *Chemical Record* 23 (2023): e202300063.
2. S. K. Ghosh, "Efficient Catalytic Methods for Asymmetric Cross-Aldol Reaction of Aldehydes," *ChemistrySelect* 9 (2024): e202304539.
3. P. Saini, Jyoti, P. K. Sharma, and V. Singh, " β -halovinyl Aldehydes: Multifaceted Versatile Building Blocks in Organic Synthesis," *European Journal of Organic Chemistry* 28 (2025): e202401058.
4. K. Reimer and F. Tiemann, "Ueber die Einwirkung von Chloroform auf Alkalische Phenolate," *Berichte der Deutschen Chemischen Gesellschaft* 9 (1876): 824–828.
5. L. Gattermann and J. A. Koch, "Eine Synthese Aromatischer Aldehyde," *Berichte der Deutschen Chemischen Gesellschaft* 30 (1897): 1622–1624.
6. A. Vilsmeier and A. Haack, "Über die Einwirkung von Halogenphosphor auf Alkyl-formanilide. Eine Neue Methode zur Darstellung Sekundärer und Tertiärer *p*-Alkylamino-benzaldehyde," *Berichte der Deutschen Chemischen Gesellschaft* 60 (1927): 119–122.
7. J. C. Duff and E. J. Bills, "Reactions between Hexamethylenetetramine and Phenolic Compounds. Part I. A New Method for the Preparation of 3- and 5-Aldehydosalicylic Acids," *Journal of the Chemical Society* (1932): 1987.
8. C. Zhu, T. Pinkert, S. Greßies, and F. Glorius, "One-Pot C–H Formylation Enabled by Relay Catalysis of Manganese(I) and Iron(III)," *ACS Catalysis* 8 (2018): 10036–10042.
9. M. Shigeno, Y. Fujii, A. Kajima, K. Nozawa-Kumada, and Y. Kondo, "Catalytic Deprotonative α -Formylation of Heteroarenes by an Amide Base Generated in Situ from Tetramethylammonium Fluoride and Tris(trimethylsilyl)amine," *Organic Process Research & Development* 23 (2019): 443–451.
10. J. Dong, X. Wang, H. Song, Y. Liu, and Q. Wang, "Photoredox-Catalyzed Redox-Neutral Minisci C–H Formylation of *N*-Heteroarenes," *Advanced Synthesis & Catalysis* 362 (2020): 2155–2159.
11. V. Aomchad, À. Cristófol, F. D. Monica, B. Limburg, V. D'Elia, and A. W. Kleij, "Recent Progress in the Catalytic Transformation of Carbon Dioxide into Biosourced Organic Carbonates," *Green Chemistry* 23 (2021): 1077–1113.
12. D. A. Sable, K. S. Vadagaonkar, A. R. Kapdi, and B. M. Bhanage, "Carbon Dioxide Based Methodologies for the Synthesis of Fine Chemicals," *Organic & Biomolecular Chemistry* 19 (2021): 5725–5757.
13. R. Cauwenbergh, V. Goyal, R. Maiti, K. Natte, and S. Das, "Challenges and Recent Advancements in the Transformation of CO₂ into Carboxylic Acids: Straightforward Assembly with Homogeneous 3d Metals," *Chemical Society Reviews* 51 (2022): 9371–9423.
14. S. Yao, J. He, F. Gao, et al., "Highly Selective Semiconductor Photocatalysis for CO₂ Reduction," *Journal of Materials Chemistry A* 11 (2023): 12539–12558.
15. Q.-W. Song, R. Ma, P. Liu, K. Zhang, and L.-N. He, "Recent Progress in CO₂ Conversion into Organic Chemicals by Molecular Catalysis," *Green Chemistry* 25 (2023): 6538–6560.
16. T. Ema, "Selective Conversions of CO₂ into Value-Added Chemicals via Cooperative Catalysis Using Multifunctional Catalysts," *Bulletin of the Chemical Society of Japan* 96 (2023): 693–701.
17. W. Natongchai, D. Crespy, and V. D'Elia, "CO₂ Fixation: Cycloaddition of CO₂ to Epoxides Using Practical Metal-Free Recyclable Catalysts," *Chemical Communications* 61 (2025): 419–440.
18. Y. Yang and J.-W. Lee, "Toward Ideal Carbon Dioxide Functionalization," *Chemical Science* 10 (2019): 3905–3926.
19. C.-K. Ran, X.-W. Chen, Y.-Y. Gui, et al., "Recent Advances in Asymmetric Synthesis with CO₂," *Science China Chemistry* 63 (2020): 1336–1351.
20. X. He, L.-Q. Qiu, W.-J. Wang, K.-H. Chen, and L.-N. He, "Photocarboxylation with CO₂: An Appealing and Sustainable Strategy for CO₂ Fixation," *Green Chemistry* 22 (2020): 7301–7320.
21. I. Dutta, S. S. Gholap, M. M. Rahman, et al., "Homogeneous Catalysis in *N*-Formylation/*N*-Methylation Utilizing Carbon Dioxide as the C1 Source," *Chemistry – An Asian Journal* 19 (2024): e202400497.
22. Q. Yuan, X. Cai, W. Ding, and Y. Zhu, "Recent Advances in *N*-Formylation Reaction for the Chemical Recycling of Carbon Dioxide," *Green Chemistry* 26 (2024): 11106–11124.
23. W.-H. Wang, Y. Himeda, J. T. Muckerman, G. F. Manbeck, and E. Fujita, "CO₂ Hydrogenation to Formate and Methanol as an Alternative to Photo- and Electrochemical CO₂ Reduction," *Chemical Reviews* 115 (2015): 12936–12973.
24. F. J. Fernández-Alvarez and L. A. Oro, "Homogeneous Catalytic Reduction of CO₂ with Silicon-Hydrides, State of the Art," *ChemCatChem* 10 (2018): 4783–4796.
25. R. A. Pramudita and K. Motokura, "Transformative Reduction of Carbon Dioxide through Organocatalysis with Silanes," *Green Chemistry* 20 (2018): 4834–4843.
26. Y. Zhang, T. Zhang, and S. Das, "Catalytic Transformation of CO₂ into C1 Chemicals Using Hydrosilanes as a Reducing Agent," *Green Chemistry* 22 (2020): 1800–1820.
27. S. Bontemps, "Boron-Mediated Activation of Carbon Dioxide," *Coordination Chemistry Reviews* 308 (2016): 117–130.
28. S. N. Riduan, Y. Zhang, and J. Y. Ying, "Conversion of Carbon Dioxide into Methanol with Silanes over *N*-Heterocyclic Carbene Catalysts," *Angewandte Chemie International Edition* 48 (2009): 3322–3325.
29. D. Mukherjee, D. F. Sauer, A. Zanardi, and J. Okuda, "Selective Metal-Free Hydrosilylation of CO₂ Catalyzed by Triphenylborane in Highly Polar, Aprotic Solvents," *Chemistry – A European Journal* 22 (2016): 7730–7733.
30. M. Rauch and G. Parkin, "Zinc and Magnesium Catalysts for the Hydrosilylation of Carbon Dioxide," *Journal of the American Chemical Society* 139 (2017): 18162–18165.
31. M. Rauch, Z. Strater, and G. Parkin, "Selective Conversion of Carbon Dioxide to Formaldehyde via a Bis(silyl)acetal: Incorporation of Isotopically Labeled C₁ Moieties Derived from Carbon Dioxide into Organic Molecules," *Journal of the American Chemical Society* 141 (2019): 17754–17762.
32. H. H. Cramer, B. Chatterjee, T. Weyhermüller, C. Werlé, and W. Leitner, "Controlling the Product Platform of Carbon Dioxide Reduction: Adaptive Catalytic Hydrosilylation of CO₂ Using a Molecular Cobalt(II) Triazine Complex," *Angewandte Chemie International Edition* 59 (2020): 15674–15681.
33. F. Ritter, T. P. Spaniol, I. Douair, L. Maron, and J. Okuda, "Molecular Zinc Hydride Cations [ZnH]⁺: Synthesis, Structure, and CO₂ Hydrosilylation Catalysis," *Angewandte Chemie International Edition* 59 (2020): 23335–23342.

34. H. H. Cramer, S. Ye, F. Neese, C. Werlé, and W. Leitner, "Cobalt-Catalyzed Hydrosilylation of Carbon Dioxide to the Formic Acid, Formaldehyde, and Methanol Level. How to Control the Catalytic Network?," *JACS Au* 1 (2021): 2058–2069.
35. D.-Y. Zhu, L. Fang, H. Han, Y. Wang, and J.-B. Xia, "Reductive CO₂ Fixation via Tandem C–C and C–N Bond Formation: Synthesis of Spiro-Indolepyrrolidines," *Organic Letters* 19 (2017): 4259–4262.
36. D.-Y. Zhu, W.-D. Li, C. Yang, J. Chen, and J.-B. Xia, "Transition-Metal-Free Reductive Deoxygenative Olefination with CO₂," *Organic Letters* 20 (2018): 3282–3285.
37. Y. Zhao, X. Guo, X. Ding, et al., "Reductive CO₂ Fixation via the Selective Formation of C–C Bonds: Bridging Enaminones and Synthesis of 1,4-Dihydropyridines," *Organic Letters* 22 (2020): 8326–8331.
38. Y. Zhao, X. Liu, L. Zheng, et al., "One-Pot Methylenation–Cyclization Employing Two Molecules of CO₂ with Arylamines and Enaminones," *The Journal of Organic Chemistry* 85 (2020): 912–923.
39. W.-D. Li, J. Chen, D.-Y. Zhu, and J.-B. Xia, "Fe-Catalyzed Pictet-Spengler-Type Cyclization via Selective Four-Electron Reductive Functionalization of CO₂," *Chinese Journal of Chemistry* 39 (2021): 614–620.
40. S. Xiang, W. Fan, W. Zhang, Y. Li, S. Guo, and D. Huang, "Aqueous CO₂ Fixation: Construction of Pyridine Skeletons in Cooperation with Ammonium Cations," *Green Chemistry* 23 (2021): 7950–7955.
41. K. Takaishi, H. Kosugi, R. Nishimura, Y. Yamada, and T. Ema, "C-Methylenation of Anilines and Indoles with CO₂ and Hydrosilane Using a Pentanuclear Zinc Complex Catalyst," *Chemical Communications* 57 (2021): 8083–8086.
42. T. Murata, M. Hiyoshi, S. Maekawa, et al., "Deoxygenative CO₂ Conversions with Triphenylborane and Phenylsilane in the Presence of Secondary Amines or Nitrogen-Containing Aromatics," *Green Chemistry* 24 (2022): 2385–2390.
43. K. Takaishi, R. Nishimura, Y. Toda, H. Morishita, and T. Ema, "One-Pot Synthesis of Dihydropyrans via CO₂ Reduction and Domino Knoevenagel/Oxa-Diels–Alder Reactions," *Organic Letters* 25 (2023): 1370–1374.
44. K. Takaishi, H. Morishita, K. Iwaki, and T. Ema, "Deoxygenative Dual CO₂ Conversions: Methylenation and Switchable N-Formylation/N-Methylation of Tryptamines," *Green Chemistry* 27 (2025): 5359–5365.
45. B. Yu, Y. Zhao, H. Zhang, et al., "Pd/C-Catalyzed Direct Formylation of Aromatic Iodides to Aryl Aldehydes Using Carbon Dioxide as a C1 Resource," *Chemical Communications* 50 (2014): 2330–2333.
46. B. Yu, Z. Yang, Y. Zhao, et al., "An Efficient and General Method for Formylation of Aryl Bromides with CO₂ and Poly(methylhydrosiloxane)," *Chemistry – A European Journal* 22 (2016): 1097–1102.
47. Z. Liu, Z. Yang, B. Yu, et al., "Rhodium-Catalyzed Formylation of Aryl Halides with CO₂ and H₂," *Organic Letters* 20 (2018): 5130–5134.
48. D. Li, L. Wei, W. Xiong, H. Jiang, and C. Qi, "Palladium-Catalyzed Reductive Formylation of Aryl Iodides with CO₂ under Mild Conditions," *The Journal of Organic Chemistry* 88 (2023): 5231–5237.
49. X. Ren, Z. Zheng, L. Zhang, Z. Wang, C. Xia, and K. Ding, "Rhodium-Complex-Catalyzed Hydroformylation of Olefins with CO₂ and Hydrosilane," *Angewandte Chemie International Edition* 56 (2017): 310–313.
50. K. Hua, X. Liu, B. Wei, et al., "Chemo- and Regioselective Hydroformylation of Alkenes with CO₂/H₂ over a Bifunctional Catalyst," *Green Chemistry* 23 (2021): 8040–8046.
51. R. Sang, Y. Hu, R. Razzaq, et al., "A Practical Concept for Catalytic Carbonylations Using Carbon Dioxide," *Nature Communications* 13 (2022): 4432.
52. Y. Li, S. Song, and S. M. Sadeghzadeh, "Ruthenium Nanocatalysts Immobilized on DFNS-IL Heterogeneous Catalyst for Hydroformylation of Alkenes with CO₂ and H₂," *Catalysis Letters* 153 (2023): 95–103.
53. A.-G. Wu, J. Ding, L. Zhao, H.-R. Li, and L.-N. He, "Hydroformylation of Olefins with CO₂/H₂ and Hydrosilane by Copper/Cobalt Tandem Catalysis," *ChemSusChem* 17 (2024): e202400608.
54. T. Murata, M. Hiyoshi, M. Ratanasak, J. Hasegawa, and T. Ema, "Synthesis of Silyl Formates, Formamides, and Aldehydes via Solvent-Free Organocatalytic Hydrosilylation of CO₂," *Chemical Communications* 56 (2020): 5783–5786.
55. K. Nakaoka, C. Guo, Y. Saiki, S. Furukawa, and T. Ema, "Synthesis of Enamines, Aldehydes, and Nitriles from CO₂: Scope of the One-Pot Strategy via Formamides," *The Journal of Organic Chemistry* 88 (2023): 15444–15451.
56. F. Yang, Y. Saiki, K. Nakaoka, and T. Ema, "One-Pot Synthesis of Aldehydes or Alcohols from CO₂ via Formamides or Silyl Formates," *Advanced Synthesis & Catalysis* 365 (2023): 877–883.
57. J. F. W. McOmie and D. E. West, "3,3'-Dihydroxybiphenyl," *Organic Syntheses* 49 (1969): 50–52.
58. S. Okaya, K. Okuyama, K. Okano, and H. Tokuyama, "Trichloroboron-Promoted Deprotection of Phenolic Benzyl Ether Using Pentamethylbenzene as a Non Lewis-Basic Cation Scavenger," *Organic Syntheses* 93 (2016): 63–74.
59. H. Wu, B. Liu, K. Yang, et al., "Synthesis and Biological Evaluation of FICZ Analogues as Agonists of Aryl Hydrocarbon Receptor," *Bioorganic & Medicinal Chemistry Letters* 30 (2020): 126959.
60. S. Li, S. Nakahara, T. Adachi, T. Murata, K. Takaishi, and T. Ema, "Skeletal Formation of Carbocycles with CO₂: Selective Synthesis of Indolo[3,2-*b*]carbazoles or Cyclophanes from Indoles, CO₂, and Phenylsilane," *Journal of the American Chemical Society* 146 (2024): 14935–14941.
61. L. F. Fieser, J. L. Hartwell, J. E. Jones, J. H. Wood, and R. W. Bost, "9-Anthraldehyde; 2-Ethoxy-1-naphthaldehyde," *Organic Syntheses* 20 (1940): 11–13.
62. H.-P. Shi, L.-W. Shi, J.-X. Dai, et al., "Synthesis, Photophysical and Electrochemical Properties and Theoretical Studies on Three Novel Indolo[3,2-*b*]carbazole Derivatives Containing Benzothiazole Units," *Tetrahedron* 68 (2012): 9788–9794.
63. V. S. Kadam, P. A. Bhatt, H. S. Karmakar, S. S. Zade, and A. L. Patel, "Benzimidazole-Substituted Indolo[3,2-*b*]carbazoles: Acid-Responsive Probes," *ChemistrySelect* 4 (2019): 3948–3952.
64. T. Mizutani, T. Ema, T. Yoshida, Y. Kuroda, and H. Ogoshi, "Recognition of α -Amino Acid Esters by Zinc Porphyrin Derivatives via Coordination and Hydrogen Bonding Interactions. Evidence for Two-Point Fixation from Thermodynamic and Induced Circular Dichroism Spectroscopic Studies," *Inorganic Chemistry* 32 (1993): 2072–2077.
65. Y. Okabe, S. K. Lee, M. Kondo, and S. Masaoka, "Syntheses and CO₂ Reduction Activities of π -Expanded/Extended Iron Porphyrin Complexes," *Journal of Biological Inorganic Chemistry* 22 (2017): 713–725.

Supporting Information

Additional supporting information can be found online in the Supporting Information section. Experimental procedures, compound data, and DFT calculations.